Polymer Chemistry

Accepted Manuscript

ROYAL SOCIETY OF CHEMISTRY

www.rsc.org/polymers

Polymer Chemistry

RSCPublishing

ARTICLE

Cite this: DOI: 10.1039/x0xx00000x
Received 00th January 2013,
Accepted 00th January 2013
DOI: 10.1039/x0xx00000x
www.rsc.org/

Camptothecin prodrug block copolymer micelles with high drug loading and target specificity

Adnan R Khan[a,c,d], Johannes Pall Magnusson[a], Sue Watson[b], Anna Grabowska[b], Robert W. Wilkinson[c], Cameron Alexander[a] and David Pritchard[a]

The clinical efficacy of cytotoxic drugs in the treatment of cancer is often hampered by poor pharmacodynamics and systemic toxicity. Here, we describe the design and synthesis of a new PEG-based system for the delivery of the cytotoxic camptothecin (CPT) into tumor cells that overexpress Leuteinizing Hormone Releasing Hormone Receptor (LHRHR). A novel functional reducible camptothecin (CPT) block copolymer conjugate was prepared using Atom Transfer Radical Polymerization (ATRP). The use of ATRP in the design and synthesis of the copolymer prodrug facilitated high drug loading and specific delivery to tumor cells. The efficacy of the polymer conjugate was evaluated in appropriate cancer cell lines in vitro. Cytotoxic potency was comparable to that of free CPT in LHRHR positive cell lines after 72 hours, whereas little cytotoxicity was observed in LHRHR negative lines. The study also evaluated the effects of polymer-based therapeutics on human peripheral blood mononuclear cells (PBMC). Free CPT demonstrated indiscriminate toxicity against the immune cells, with impairment of PBMC proliferation and a reduction in CD8+, CD4+ T cell populations. The camptothecin (CPT) block copolymer demonstrated a significant improvement in cell proliferation and maintenance of $CD8^+$ cells.

Introduction

A large number of therapeutic regimens exist for cancer treatment, many of which involve the administration of small cytotoxic drugs. The clinical efficiency of cytotoxic drugs is however often hampered by poor physical properties, difficult pharmacokinetics, immunosuppression and other adverse drug effects. Accordingly, there has been a concerted effort to deliver anti-cancer drugs in a site-specific manner, exploiting the cytotoxicity of the chemotherapeutic whilst attenuating these off-target adverse effects.[1] Polymer-based formulations are one such strategy[2-7] as these systems can increase the passive accumulation of drugs into tumors via the EPR (enhanced permeation retention) effect. [8, 9] Several *in vitro* and pre-clinical models have indicated that polymer-based therapeutics have tumor-specificity,[10, 11] with minimal accumulation in off-target sites, suggesting that such formulations may have a greater role in cancer therapy in the future. Cytotoxic drugs are incorporated onto polymers either by physical interactions or through covalent conjugation. [12-17] Both approaches do nevertheless incur certain disadvantages. Physical conjugates can release their drug payload away from the preferred site of action because of diffusion,[18] and for covalent drug-polymer conjugates, there is a compromise between obtaining sufficient drug loading and maintaining desirable solution properties. Specificity and tissue distribution can however be improved by conjugating a targeting moiety to the polymer carrier which binds to overexpressed receptors on the surface of cancer cells. [19-22] In order to maximize the potential of receptor meditated uptake it is important that the polymer carrier has an appropriate drug loading capacity since active transport mechanisms can be saturated. To address these issues we have devised a system where we use the drug as a functional part of the polymer. We have chosen the topoisomerase I inhibitor (S)-(+)-camptothecin (CPT) as an exemplar therapeutic agent. In the free drug form CPT has low water solubility, high protein binding,[23] poor stability and also exhibits adverse drug effects and a tendency to cause lymphopenia.[24, 25] In order to incorporate CPT into a polymer chain, a reducible CPT monomer was formed by conjugating the hydroxy group of CPT on to a carboxy terminus of a reducible methacrylate monomer. The shielding of the drug moiety was further improved by careful control of the polymer architecture. The polymer was synthesized using copper-mediated controlled radical polymerisation a well-established pseudo-living route to achieve the correct architecture for the block copolymer.[26] A hydrophilic Poly (poly(ethylene glycol) methacrylate) (pPEGMA) block was used to confer water solubility to the block copolymer and shield the CPT block. Our rationale for the design construct was that the block architecture intrinsically enabled high loading of CPT into the

nanoparticle core while the bioreducible linker between drug and polymer backbone minimized the exposure of CPT until it reached the reducing environment inside the cancer cell. This design suggested that once inside the cell, the polymer-CPT linker would be rapidly reduced, releasing the drug *in situ.* The added versatility of this polymer was the introduction of an acid functional initiator on the surface of the hydrophilic polymer, present on the nanoparticle exterior when the co-polymer self-assembled in aqueous solution. This allowed conjugation of a targeting LHRH peptide sequence (Gln-His-Trp-Ser-DLys(D-Cys)-Leu-Arg-Pro-NHEt-)[27] to the pPEGMA block, facilitating uptake into cells that over-express the LHRH receptor (LHRHR) such as human ovarian, breast, and prostate cancer cells.[28]

Herein, we describe a novel synthesis approach to create the high loading CPT polymer conjugate and its subsequent profiling in terms of self-assembly and stability. We tested the cytotoxicity of the conjugate against various LHRHR positive and negative cell lines (Scheme 1). We also examined the effects of the polymer against PBMC (*ex vivo*) and compared them to those of the free drug, in order to evaluate any potential immunological effects of the polymer conjugate.

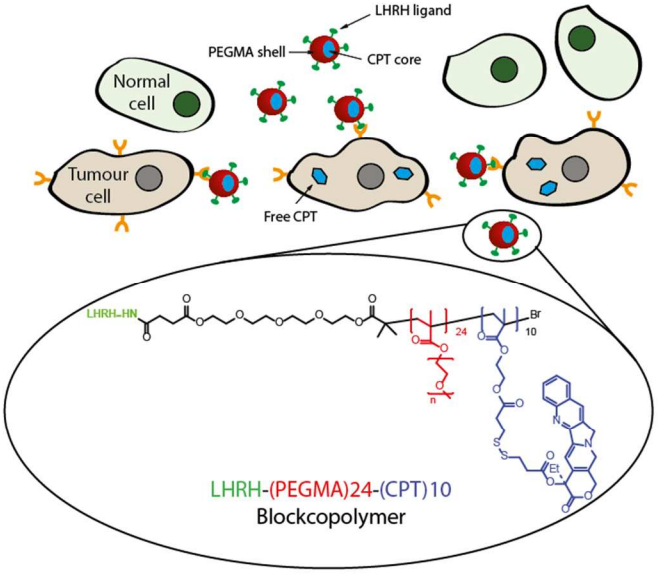

Scheme 1. Schematic representation of the targeted Camptothecin (CPT) delivery block co-polymer. Solubility and protection of the CPT core is achieved with a hydrophilic PEGMA polymer shell. Uptake and release of CPT into tumor cells is facilitated via the LHRH receptor and reducible bonds which are cleaved in the reducing environment within the cell.

Experimental section

Instrumentation.

^{1}H and ^{13}C NMR spectra were recorded on a Bruker 400 spectrometer at 399.8 MHz (^{1}H) and 100.5 MHz (^{13}C) in *d*-chloroform. All chemical shifts are reported in *ppm* relative to TMS. HRMS spectra were recorded on an ESI-TOF Waters 2795 separation module/micromass LCT platform. Fluorescence spectra were recorded using a Varian Cary Eclipse fluorescence spectrophotometer.

Molecular weights and molecular weight distributions were determined using a Varian/Polymer Laboratories GPC-50 instrument with triple detection (RI, viscometry and MALLS). Chromatograms were run at 40 °C using chloroform ($CHCl_3$) as eluent with a flow rate of 1 ml/min. The columns used were Resipore Mixed-B, detection was performed by a Refractive Index detector (RI). The machine was calibrated with linear polystyrene standards.

Centrifugation was carried out on Centaur II centrifuge at room temperature

Materials.

All solvents and reagents were of analytical or HPLC grade and purchased from Sigma or Fisher Scientific unless otherwise specified. Deuterated solvents were from Sigma Aldrich. Polyethylene glycol methyl ether (PEGMA, M*n* 475) was purchased from Sigma Aldrich and purified before use by passing it through a column filled with basic alumina. Copper (II) Bromide ($Cu(II)Br_2$, 99%), Copper (I) Bromide (Cu(I)Br, >98%), N,N′-Dicyclohexylcarbodiimide (DCC, >99%), N,N-Diisopropylethylamine (DIPEA, 99%), DL-Dithiothreitol (DTT, > 99.5%), 3,3′-Dithiodipropionic acid (>99%), 4-(Dimethylamino)pyridine (DMAP, >99%), N-(3-Dimethylaminopropyl)-N′-ethylcarbodiimide hydrochloride (EDAC, > 99%) and N,N,N′,N″,N″-Pentamethyldiethylenetriamine (PMDETA, (99%)) were used as received from Sigma Aldrich. 2-Hydroxyethyl methacrylate (HEMA, >96%) was used as received from Acros. Camptothecin (98%, CPT) was purchased from Molekula. 2-(7-Aza-1H-benzotriazole-1-yl)-1,1,3,3-tetramethyluronium hexafluorophosphate (HATU) was purchased from Fluorochem and used as received. Tris-(2-carboxyethyl)phosphine, hydrochloride (TCEP) was used as received from Invitrogen. LHRH peptide[29] was purchased from Genscript and used as received. Dialysis membrane (MWCO 1000 and 6-8K, regenerated cellulose) was used as received from Spectrapor.

Initiator synthesis.

Compound 1: (HO-TEG-Br) was synthesized and analyzed as reported previously[30]. Compound 2: *2-bromo-2-methyl-3,17-dioxo-4,7,10,13,16-pentaoxaicosan-20-oic acid* (COOH-TEG-Br). Triethylamine (0.97 g, 9.62 mmol) and Compound 1 (3 g, 8.75 mmol) were suspended in 10 mL of anhydrous MECN, the mixture was cooled down to 0 °C and under stirring succinic anhydride(0.875 g, 8.75 mmol) was added (Figure S1A). The reaction was allowed to reach room temperature and left to react for 3 hours. Subsequently the MECN was evaporated and the mixture dissolved in dichloromethane, the DCM was washed few times with water. The organic phase wash then dried with anhydrous $MgSO_4$ and removed under vacuum. The oily mixture was purified by silica column chromatography (100% Ether). The synthesis resulted in compound 2 (COOH-TEG-Br) as a pale yellow oil in 33% yield. HRMS: calcd for (M-) 442.276 found (M-) 443.003. *^{1}H NMR ($CDCl_3$, 400 MHz):*

δ 4.37-4.28 (-COOCH$_2$-, m, 4H), 3.73-3.51 (-OCH$_2$CH$_2$-, m, 12H), 2.69-2.66 (-OOC-CH$_2$-, m, 4H), 1.97-1.96 (CH$_3$-, s, 6H). ^{13}C NMR (CDCl$_3$): δ 175.87, 172.23, 171.62, 70.59-65.06 (multiple signals -OCH$_2$CH$_2$-), 55.74, 30.69, 29.08, 28.91.

Monomer synthesis.

Compound 3: *3-((3-(2-(methacryloyloxy)ethoxy)-3-oxopropyl)disulfanyl)propanoic acid* (HEMA-S-S-COOH). HEMA (1 g, 7.68 mmol) and 3,3′-dithiodipropionic acid (8.07 g, 38.4 mmol) were suspended in anhydrous THF (70 mL) and cooled down to 0 °C. (Figure S1B). Under stirring the DCC (3.17, 15.4 mmol) and DMAP (0.188 g, 1.53 mmol) were added. The mixture was allowed to reach room temperature and left to react overnight. Subsequently, the solvent was evaporated and the mixture was solubilized in DCM. The organic layer was washed repeatedly with water to remove excess of the dithiodipropionic acid. The organic layer was then dried with anhydrous $MgSO_4$ and the DCM evaporated. The residue was purified by silica column chromatography (50 Hexane / EtOAc). The synthesis resulted in compound 3 (HEMA-S-S-COOH) as an off white solid in 61% yield. *^{1}H NMR (CDCl$_3$, 400 MHz): δ 6.15 (-CH=, s, 1H), 5.62 (-CH=, s, 1H), 4.38 (-COOCH$_2$-, m, 4H), 2.93(-SCH$_2$-, m, 4H), 2.81(-OOC-CH$_2$-, m, 4H), 1.97(CH$_3$-, s, 3H). ^{13}C NMR (CDCl$_3$): δ 177.14, 171.47, 167.18, 135.85, 126.24, 62.51, 62.30, 33.94, 33.81, 32.98, 32.72, 18.28.*

Compound 4: (*S)-2-((3-((3-((4-ethyl-3,14-dioxo-3,4,12,14-tetrahydro-1H-pyrano[3',4':6,7]indolizino[1,2-b]quinolin-4-yl)oxy)-3-oxopropyl)disulfanyl)propanoyl)oxy)ethyl methacrylate* (Methacrylate-S-S-CPT). Compound 3(HEMA-S-S-COOH) (1.66 g, 5.16 mmol), EDAC (0.99 g, 5.16 mmol) and DMAP (0.07g, 0.57 mmol) were dissolved in anhydrous DCM (10mL) at 0 °C. Under stirring CPT (300 mg, 0.86 mmol) was added, the mixture was allowed to reach room temperature and left to react overnight. The next day the mixture was washed with 1N HCl solution (3 times) followed by a solution of 0.1 % $NaHCO_3$ (3 times). The organic layer was then dried with anhydrous MgSO4 and removed under vacuum. The remaining residue was purified by silica column chromatography (100 Ether → 100 DCM) to recover the purified monomer (compound 4) as yellowish powder in 84 % yield. HRMS: calcd for (M+) 653.742 found (M+) 653.159. *^{1}H NMR (CDCl$_3$, 400 MHz): δ 8.42(Ar, m, 1H), 8.25(Ar, m, 1H), 7.97(Ar, m, 1H), 7.87(Ar, m, 1H), 7.70(Ar, m, 1H), 6.14 (-CH=, m, 1H), 5.73-5.69(Ar, m, 1H), 5.61 (-CH=, m, 1H), 5.70/5.30(Ar-CH$_2$-, m, 2H), 5.30(Ar, m, 1H) 4.34 (-COOCH$_2$-, m, 4H), 3.02-2.93(-SCH$_2$-, m, 4H), 2.79-2.76 (-OOC-CH$_2$-, m, 4H), 2.34-2.30(-CH$_2$-, m, 2H), 1.96(CH$_3$-, s, 3H), 1.05-1.01(CH$_3$-, m, 3H). ^{13}C NMR (CDCl$_3$): δ 171.35, 170.71, 167.33, 167.03, 157.29, 152.89, 148.83, 146.31, 145.64, 131.17, 130.66-128.02(multiple signals, Ar,-CH=) 126.15, 120.12, 96.06, 67.03, 62.39, 62.24, 49.96, 33.89, 33.75, 33.00, 32.29, 31.77, 18.27, 7.61.*

PEGMA475 block polymer synthesis.

Compound 2 (COOH-TEG-Br) (0.15 g, 0.34 mmol), PEGMA475 (6.43 g, 13.5 mmol) and PMDETA (0.118 g, 0.68 mmol) were placed in a 2-neck round bottom flask and dissolved in toluene (14 mL). The flask was then sealed and the solution degassed with argon for 15 minutes. After 15 minutes the polymerization was initiated by the addition of Cu(I)Br (0.0485 g, 0.34 mmol) and the mixture heated up to 80 °C. After 50 minutes the polymerization was stopped by exposing the mixture to atmosphere and by cooling down. Overall monomer conversion was calculated from proton NMR spectra by comparing the vinyl proton signals from the monomers (5.6 and 6.1 *ppm*) to the overall integration across the range 3.3-3.4 ppm. In the region of 3.3-3.4 *ppm* three protons of the remaining monomer resonate as well as three protons from the polymer. Conversions were calculated by subtracting the monomer signal in the region 3.3-3.4 *ppm* from the total integration and dividing it by the total integration signal. Conversion was calculated to be 67 %. Subsequently the mixture was passed through an alumina column to remove the copper and the polymer precipitated into hexane and dried. Finally, copper traces and monomer units were removed by dialysis (MWCO 1000) in water containing small traces of EDTA. The dialysis bag was placed into pure water before lyophilization and collection of the pure polymer. After the lyophilization step 2.1 g of viscous PEGMA475 was recovered. Molecular weight was calculated by *^{1}H*-NMR by comparing the methoxy protons of the polymer (3H – δ 3.3 *ppm*) to the overall integration across the range 4.2 to 4.55 *ppm* where 2 protons of the polymer and 4 protons of the initiator resonate (Figure S2). Molecular weight was found to be 12000 by NMR, containing 24 units of PEGMA. Molecular weight and distribution were also examined by $CHCl_3$ GPC chromatography.

PEGMA-CPT block copolymer synthesis.

PEGMA475 block (0.15 g, 8.33 µmol), compound 4 (Methacrylate-S-S-CPT) (0.109 g, 167 µmol) and PMDETA (2.88 mg, 16.7 µmol) were placed in a 2-neck round bottom flask and dissolved in toluene (0.725 mL). The flask was then sealed and the solution degassed with argon for 15 minutes. After 15 minutes the polymerization was initiated by the addition of Cu(I)Br (1.195 mg, 8.33 µmmol) and the mixture heated to 80 °C. After 4 hours the polymerization was stopped by exposing the mixture to atmosphere and by cooling down. Conversion of the polymerization was verified using ^{1}H-NMR, by comparing the aromatic protons (7.7 – 8.42 *ppm*, 5H) of the methacrylate-S-S-CPT to the vinyl signal at 6.15 *ppm* (1H). Conversion was calculated to be 50 % after 4 hours polymerization. The mixture was diluted with ethanol and centrifuged at 3000 rpm to remove free Methacrylate-S-S-CPT monomer, the eluent was subsequently dialyzed in methylated spirit (MWCO 1000) to remove any remaining monomer residues. Finally the mixture was dialyzed in water containing small traces of EDTA to remove any remaining copper residues. The dialysis bag was placed into pure water before lyophilization and collection of the pure polymer. After

lyophilization 180 mg of sticky yellowish/orange PEGMA-CPT block copolymer was recovered. ^{1}H-NMR was used to confirm the complete removal of CPT monomer units. ^{1}H-NMR spectrum was also used to calculate the composition of PEGMA to CPT units, this was achieved by comparing the aromatic protons of the CPT (7.7 – 8.42ppm, 5H) to the methoxy protons (3.3 ppm, 3H) of the PEGMA macroinitiator polymer (Figure S3). Comparison of these signals revealed that for every unit of PEGMA present there were 0.4 units of CPT presents, in total ~ 10 units of CPT per polymer chain. Total molecular weight of the block copolymer was therefore 18500 g/mol by NMR. In addition molecular weight and distribution were examined by $CHCl_3$ GPC chromatography using RI detection (Resipore columns).

Conjugation of LHRH peptide to the PEGMA-CPT block copolymer.

PEGMA-CPT block copolymer (77.1 mg, 0.0042 mmol), LHRH (2.2mg, 0.0017 mmol) and HATU (2.3 mg, 0.006 mmol) were dissolved in a mixture of DCM/DMF (4 mL). The mixture was cooled down to 0°C and under stirring DIPEA was added (1.1 mg, 0.006 mmol), the solution was allowed to reach room temperature and left to react overnight. The following day the DCM was evaporated and product purified by dialysis in water (MWCO 6-8K), after dialysis the solution was lyophilized and the product recovered (77 mg). Peptide content was then evaluated using bicinchoninic acid (BCA) assay, unlabelled PEGMA-CPT block copolymer was used a blank. Polymer samples were made up in triplicate at 1 mg/mL concentration. LHRH content in polymer samples (1 mg/mL) was 26 µg/mL ± 5.4 µg/mL, which is equivalent to 2.6 % of mass of the polymer. If all of the peptide was consumed in the conjugation the mass ratio percentage should be 6.3 %, that is 41.2 % ± 8.5% of the polymer chains would have the peptide after modification. The conjugation ratio of peptide to polymer was 40.5 %, the reaction was therefore nearly quantitative in terms of coupling efficiency.

Drug release.

Drug release study was carried out under non-reducing (1X PBS pH 7.4) and reducing conditions (1X PBS, 5 mM DTT pH 7.4). Polymer 1 was dissolved in 1X PBS pH 7.4 at concentration 1 mg/mL and diluted with the appropriate buffer 10 times. 5 mL of each solution was placed inside a dialysis bag MWCO 6-8K and placed into a beaker containing 200 mL of the appropriate buffer at 37 °C, 1 mL samples were taken at appropriate time points from the beaker and replaced with 1 mL of fresh buffer. Each experiment was carried out in triplicate. Samples were read on fluorescence spectrophotometer using 370 nm excitation and 430 nm emission. Total drug content was determined by using TCEP as the reducing agent and the value attained using TCEP was set as 100 % release.

Cell culture – Cytotoxicity assay.

The human ovarian carcinoma cell line A2780, the human colon adenocarcinoma cell line CACO-2 and the human lung adenocarcinoma, CALU-3 cell line were obtained from the ECACC. The human ovarian adenocarcinoma cell line IGROV-1 was kindly donated by the Marco Negri Institute, Milan, Italy. Cells were seeded on 96-well plates at 1 x 10^4/well. Cells were then treated with a concentration range (0 – 100 µM) of CPT or Polymer 1, with the equivalent amount of DMSO or PBS used as vehicle controls. Treatment duration was 72 hours. After treatment of cells 10 µl of 5 mg/mL MTT solution (Sigma) was added to each well. The plates were incubated for 4 hours at 37 °C and formazan crystals were dissolved by the addition of isopropanol. Absorbance was measured at 570 nm. The percentage of cell viability was calculated using untreated cells as a maximal proliferation and repeatedly freeze-thawed cells as minimal proliferation.

Competitive inhibition of Polymer 1 by LHRH.

Cells were seeded as described above. A2780 and IGROV-1 cells were incubated simultaneously with 10 µM LHRH peptide (GenScript) and a concentration range of Polymer 1 (equivalent to 0 – 100 µM CPT). Assays ran for 72 hours. Cell viability was measured by the MTT assay as described above, percentage of cell viability was calculated using untreated cells as a maximal proliferation and repeatedly freeze-thawed cells as minimal proliferation. To calculate IC_{50} values, cell viability data were normalized against controls and fitted to a variable slope model.

PBMC Proliferation assay.

Peripheral blood was obtained from healthy donors in accordance with local ethical committee approval (EC# BT/04/2005). Peripheral blood mononuclear cells (PBMC) were separated via a density-gradient centrifugation over Histopaque-1077 (Sigma) twice as before, firstly to isolate PBMCs with the second density gradient used for the removal of platelets. The resultant cells were then washed in isolation buffer containing phosphate buffered saline (PBS) + 1 % w/v bovine serum albumin (BSA) (Sigma) + 1 mM EDTA (Sigma) before viability counting via Trypan Blue exclusion (Fluka). 1 x 10^5/well PBMC cells were stimulated with 10 µg/ml phytohemagglutinin (PHA) (Sigma). The final volume was adjusted to 200 µl using cell media. After 72 hours, 100 µl of cell supernatant was taken and stored at – 40 ˚C. Cells were then either stained for viability using Propidium Iodide (Sigma) or pulsed with 1 µCi of [3H]-labelled thymidine per well (TRA120, Amersham). The plate was left to incubate for a further 18 hours before being harvested onto a microscintillation plate (Perkin-Elmer). After repeated washes with de-ionised water, the plate was allowed to dry for an hour. 20 µl of scintillation fluid (Microscint 0, Perkin-Elmer) was added per well before the plate was covered with optical tape (Perkin Elmer). Thymidine incorporation was quantified using a Packard TopCount NXT Microplate Scintillation counter.

Flow Cytometry

Cells were stained with cell surface markers CD3-PE (UCHT1, eBioscience), CD4-ECD (SFCI12T4D11 - Beckman Coulter),

CD8-FITC (HIT8a – BioLegend) CD25-PE (BC96 - BioLegend). Cells were incubated with fluorochrome-conjugated antibodies for 15 minutes before fixation with 3 % v/v formaldehyde (Sigma). Cells were then permabilised using Foxp3 Perm Buffer (BioLegend) before incubation with Foxp3-AlexaFluor488 (Clone 259D – BioLegend) for 30 min. Cells were then resuspended in FACS wash buffer (BioLegend) and read via a Beckman Coulter FC 500 flow cytometer. Analysis involved gating on lymphocyte populations from forward/side-scatter plots before selecting regions of interest. To detect the expression of LHRHR on the cell surface of IGROV-1, A2780, CACO-2 and CALU-3, indirect immunofluorescence staining was performed. Cells were incubated with Rabbit Polyclonal LHRHR (Abcam) (500 ng/mL) or a Rabbit polyclonal IgG isotype control (Sigma) (500 ng/mL) for 20 minutes. After washing, cells were incubated with a goat anti-rabbit-FITC IgG (Sigma) for 30 minutes in the dark. The cells were washed again and re-suspended for analysis via flow cytometry. For Propidium Iodide Live/Dead cell sorting, treated PBMC were washed in PBS + 0.1 % BSA before being incubated with 2 µg/ml Propidium Iodide for 5 minutes. Cells were then washed and sorted by the MoFloXDP flow cytometer. Cells that were negative for Propidium Iodide were sorted into tubes for phenotyping. Weasel 3.0 software for Windows was used for the analysis of the results.

Statistical Analysis.

The results are given as mean ± SD. Statistical analysis was performed with Graphpad Prism 5 software using a Tukey's Multiple comparison test for all results, where a student's t test was performed. $P \leq 0.05$ was considered significant.

Results and Discussions

Synthesis

The CPT monomer was synthesized in 2 steps (Figure S1B, Compound 4) Dithiodipropionic acid was first reacted with 2-hydroxyethyl methacrylate (HEMA) monomer to create an acid functional monomer containing a reducible disulfide bond. The acid side chain of this monomer was in turn coupled to the hydroxyl group of CPT to form the reducible CPT monomer (Compound 4). The addition of a hydrophobic moiety to the 20S position on CPT was designed to improve the stability of the lactone towards hydrolysis and decrease the activity under non reducing conditions.[31] The block copolymer architecture was intended to strengthen these traits further, keeping the CPT concealed away inside the core of the polymer macro structure therefore preventing hydrolysis, protein serum binding [23] and unwanted target binding. An acid functional (ATRP) initiator was synthesized (Figure S1, Compound 2) with a tetraethyleneglycol (TEG) spacer between the polymerization initiating functionality and the acid terminus to ensure good control during subsequent polymerization.[32] The hydrophilic PEGMA block was grown first to ensure that the LHRH peptide would be accessible on the surface of the polymer after conjugation.

Overall, monomer conversion was calculated from proton NMR spectra (Figure S2) that indicated the polymer contained on average 24 units of PEGMA, therefore giving it an average size of 12000 Da. The purified PEGMA block copolymer was then used as a macroinitiator to initiate the polymerization of the CPT block (Figure 1).

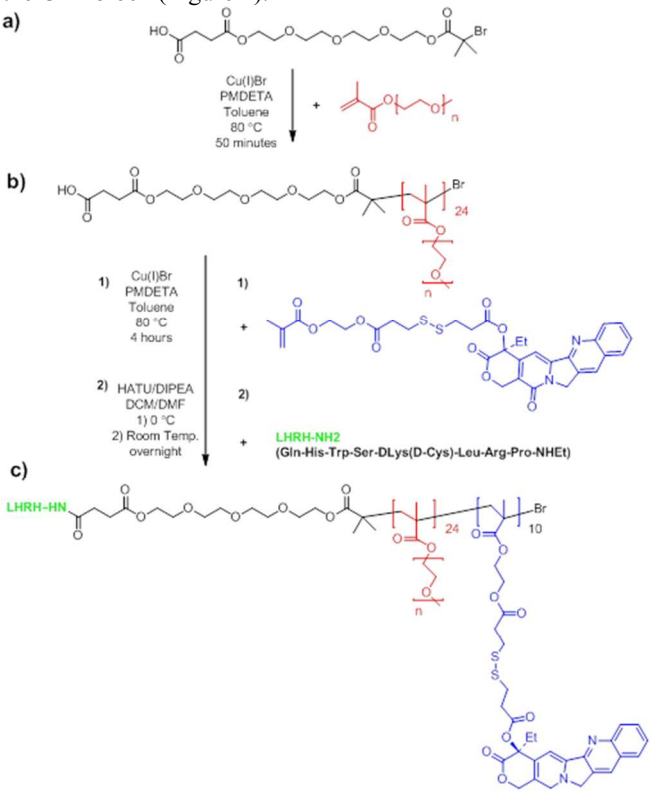

Figure 1. Synthesis route for the LHRH functional PEGMA-CPT block-copolymer. a) Synthesis of hydrophilic PEGMA block from acid functional ATRP initiator. b) 1) Synthesis of PEGMA-CPT block copolymer. 2) Conjugation of the LHRH sequence to the free acid terminus. c) Chemical structure of polymer 1.

The composition of the block copolymer was determined by ^{1}H NMR spectroscopy. Peak integrals indicated that the polymer contained ~10 monomer drug units in the CPT block per 24 units of the PEGMA based macromonomer. The total average molecular weight per chain was calculated to be 18500 Da (Figure S3). Gel permeation chromatography (GPC) in chloroform indicated molar masses in relatively good agreement with those derived from NMR however the addition of the CPT block decreased the size slightly according to GPC in chloroform. GPC of the same polymer using water as the eluent suggested self-assembly, as the polymer eluted at a much higher apparent molar mass compared to the water-soluble macroinitiator precursor and the block copolymer in chloroform, a clear indication that the PEGMA block had successfully initiated the polymerization of the second block. The free acid terminus of the block copolymer was subsequently successfully conjugated to a known LHRH peptide[14] to form Polymer 1. We aimed for ~ 50% end-group modifications of the polymer since it has been previously

shown that a high ligand density at a surface can hinder access at receptors and reduce receptor mediated uptake.[33] Assays of peptide content after conjugation demonstrated that functionalization relative to the polymer was 41.2% ±8.5%. As a negative control the acid terminus of the polymer was capped with methylamine to form Polymer 2.

Table 1. Polymer characteristics: a) Theoretical, calculated from monomer/initiator ratio and conversion. b) From GPC ($CHCl_3$,poly(styrene) standards). c) NMR integrals, calculated from ratio of monomer to initiator and PEGMA to CPT in the NMR spectrums. d) total CPT (free drug) content in block copolymer.

Polymer	$M_{n\ Th}$[a]	M_n-GPC[b]	M_w/M_n[b]	M_n NMR[c]	% CPT[d]
PEGMA macro initiator	13200	17200	1.2105	12000	-----
PEGMA-CPT block copolymer	16350	15500	1.3407	18500	18.3%

The self-assembly behaviour of the block copolymer was verified with dynamic light scattering (DLS) and by determining the critical aggregation concentration (CAC) (Figure S4). DLS analysis revealed that the polymer drug conjugate self assembled into discrete objects with a radius of hydration around 20 nm in isotonic PBS buffer. (Figure S4). A small population of larger objects (R_h ~ 100 nm) was observed in the intensity distributions obtained via DLS, but these were not apparent in TEM (Figure S6). This suggests that larger particles were low in number, and likely arose from low frequency aggregation events. The release profile of CPT from the polymer was examined in isotonic PBS under non-reducing and simulated reducing conditions (5 mM DTT). Under reducing conditions 90 % release of CPT was achieved after 24 hours while in a non-reducing environment less than 10 % release was achieved in the same time (Figure 2). Change of medium from PBS to fetal calf serum (FCS) did not significantly affect CPT release either (Figure S5), indicating that the block co-polymer was not subject to significant ester side-chain hydrolysis and release of CPT via a non-reductive pathway over the 24 hr time period.

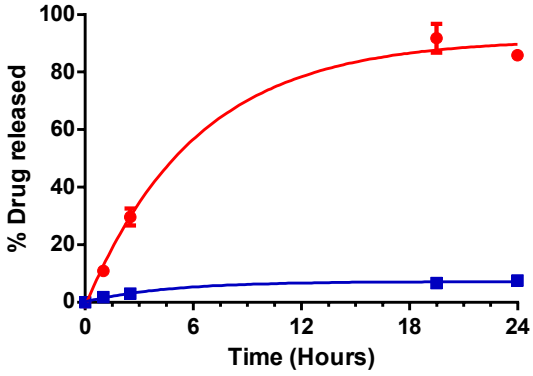

Figure 2. Induction of CPT release via reduction of disulfide linker. CPT release from Polymer 1 in PBS buffer pH 7.4 (●) and in presence of 5 mM DTT (■) over 24 hours. Error bars represent standard deviation. Statistical significance determined by a one-way ANOVA analysis with column comparisons using Tukey's Multiple Comparison Test (* = $p < 0.05$).

Targeting of LHRHR high expressing cells

With flow cytometry the expression of LHRHR was evident on A2780, IGROV-1 and CACO-2 with low expression detected in CALU-3 (Figure 3). The expression seen on these cells correlates with existing data in both ovarian and lung cells[34]. However, LHRHR is expressed at significantly higher levels in ovarian tissue compared to other cell types[35]. The cytotoxicity of Polymer 1 against a variety of cell lines was assessed in order to ascertain whether this type of delivery system would be useful as part of a treatment stratagem.

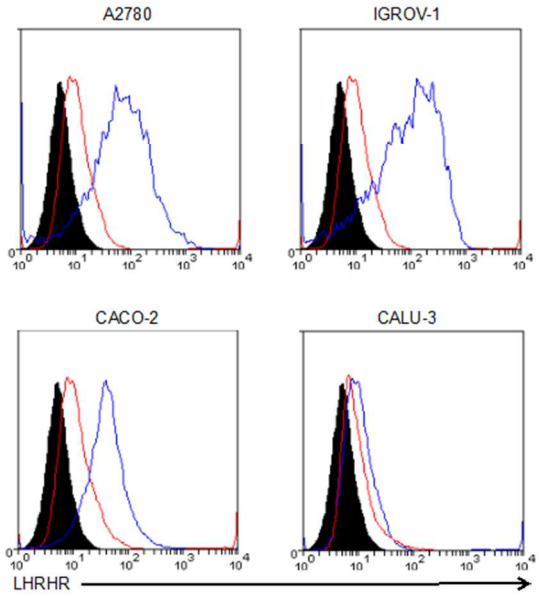

Figure 3. Expression of LHRHR on cancer cells via flow cytometry. Cell lines A2780, IGROV-1, CACO-2 and CALU-3 were assessed for LHRHR expression (blue) compared to isotype (red) and unstained cells.

The efficiency of the CPT polymer was evaluated by comparing its CPT activity relative to native CPT. The activities of the monomer or the product from reduction of the disulfide-linked CPT (i.e. CPT 3-mercaptopropanoate) were not evaluated but from the QSAR studies on CPT[31] it can be assumed that the modification would decrease activity in comparison to native CPT. The comparison of cytotoxicity data between polymer-CPT conjugates and free CPT is thus biased in favour of the free drug as opposed to the CPT-derivative released on reduction.

In Figure 4 the cytotoxic effect of Polymer 1(CPT/PEGMA/LHRH), Polymer 2 (CPT/PEGMA) and CPT is demonstrated against the cell lines A2780, CACO-2, CALU-3 and IGROV-1 at 72 hours. In cell lines that express high levels of LHRHR (A2780 and IGROV-1) the potency of Polymer 1 was comparable to that of native drug at 72 hours. The potency of Polymer 1 correlated with expression of LHRHR on the cell surface (IGROV-1 > A2780 > CACO-2 > CALU-3) suggesting that the effects seen were LHRHR dependent.

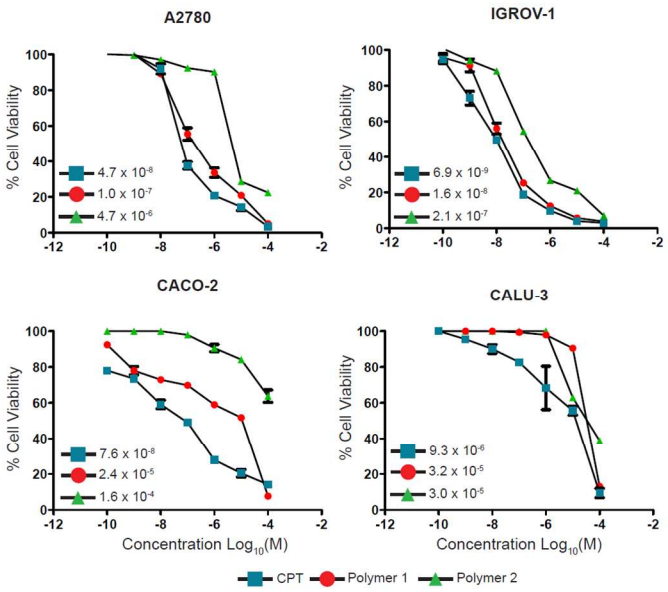

Figure 4. Cytotoxicity of compounds on cancer cell lines. Cytotoxicity of Polymer 1 (LHRH) (●), Polymer 2 (methylamine capped) (▲) and CPT (■) at 72 hours on ovarian cell lines; A2780 and IGROV-1 (LHRHRhigh), colon cell line CACO-2 and lung cell line CALU-3 (LHRHRlow). IC50 values are also depicted in Molar. Figure representative of three independent experiments. Error bars represent standard deviation.

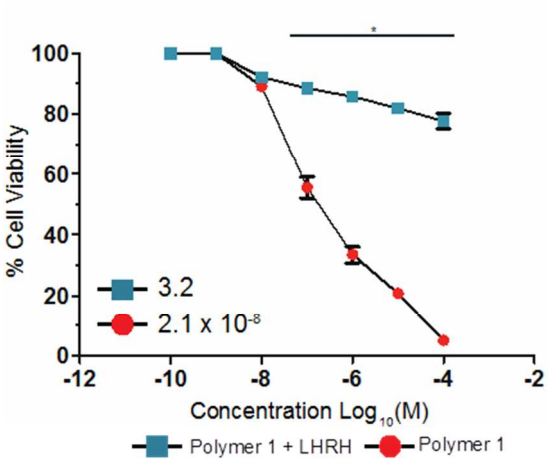

Figure 5. LHRH peptide blocks Polymer 1 demonstrating uptake is via LHRHR. Cytotoxicity of Polymer 1 (●) was compared to Polymer 1 incubated with 10 μM LHRH on the A2780 cancer cell line (■) 72 hours. IC50 values are also presented. Figure representative of three independent experiments. Error bars represent standard deviation. Statistical significance determined by a one-way ANOVA analysis with column comparisons using Tukey's Multiple Comparison Test. (* = p <0.05)

Comparing the cytotoxicity of Polymer 1 against Polymer 2 provided confirmation of this observation. The lack of targeting ligand reduced the efficacy of the construct (IGROV-1, Polymer 2 vs. Polymer 1, IC_{50} (M) 2.1x 10^{-7} vs. 1.6 x 10^{-8}, n = 3; $p < 0.05$). The change in potency of Polymer 1 supported the proposed mechanism of site-specific targeting. The potency of free CPT decreases over time, due to protein binding and hydrolysis of the drug to its sodium salt, which displays up to a 90 % reduction in activity compared to the parent drug as previously described.[36]

In order to investigate whether the activity of Polymer 1 was primarily dependent on LHRHR mediated uptake, IGROV-1 cells were treated with a combination of 10 μM LHRH and a concentration range (0 – 100 μM) of Polymer 1 before measuring cytotoxicity over a period of 72 hours as a functional readout of uptake. Figure 5 illustrates the effect of added free LHRH on inhibition of cytotoxicity of Polymer 1. At 72 hours, addition of exogenous LHRH significantly restricted Polymer 1-mediated cytotoxicity (Polymer 1 + LHRH vs. Polymer 1; IC_{50} (M) 3.2 vs. 2.1 x 10-8, n = 3; $p < 0.05$). The competitive binding experiments thus established that the cytotoxic effect of Polymer 1 was primarily mediated by receptor internalization.

Having established that Polymer 1 has LHRHR specific properties, there was also a small percentage of CPT released in a non-receptor mediated manner due to hydrolysis (see Figure 2). Due to the intimate relationship between the immune system and the tumor, any treatment of cancerous cells will almost certainly have immunological consequences. To study the effect of CPT and Polymer 1 on the immune population, healthy donor derived PBMC (peripheral blood mononuclear cells) were divided into stimulated and non-stimulated groups (stimulation provided with the T cell mitogen, phytohemagglutinin, PHA) and treated with Polymer 1 or CPT over a concentration range (0 – 100 μM) for 72 hours. PHA was used as a means to provide a robust, reproducible proliferative response as opposed to antigenic stimulation, which can be donor dependent. The duration of this assay was selected since at this time the IC_{50} of both Polymer 1 and CPT were similar in cytotoxicity assays as apparent from Figure 4.

The change in the stimulation index seen on addition of each compound is shown in Figure 6. The stimulation index, i.e the mean counts per minute (CPM) of mitogen-stimulated cells divided by the mean CPM of cells cultured without mitogen, allows for comparison of both stimulated and non-stimulated experimental groups. From Figure 6 it is clear that CPT almost completely abrogated stimulated PBMC proliferation (0.01 – 100 μM, n = 3; $p < 0.05$). In comparison, Polymer 1 demonstrated a dose-dependent effect with doses of 1 μM and higher causing a significant decrease in cell proliferation (1 – 100 μM, n = 3; $p < 0.05$). A similar trend was seen in the non-stimulated groups, whereby free CPT demonstrated a significant reduction in cell proliferation, albeit to a lesser extent compared to when incubated with the stimulated group. The marked changes in the stimulation index between

experimental groups are due to the affinity of CPT and the prodrug CPT for proliferating cells.[37]

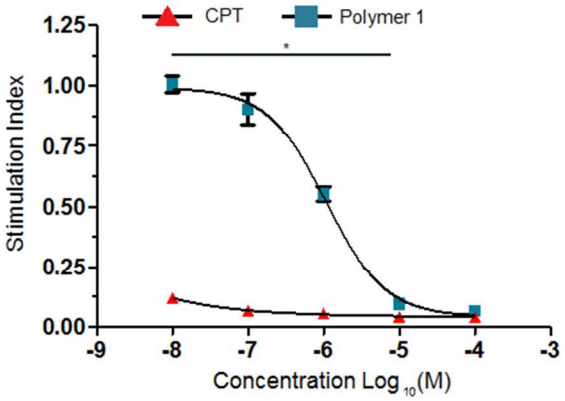

Figure 6. Effect of Polymer 1 (■)and CPT (▲) on PBMC. PBMC were stimulated with PHA for 72 hours. Stimulation index calculated by division of mean counts per minute (CPM) of stimulated cells by CPM of unstimulated cells. Figures representative of three independent experiments. Error bars represent standard deviation. Statistical significance determined by a one-way ANOVA analysis with column comparisons using Tukey's Multiple Comparison Test (* = $p < 0.05$).

The role of chemotherapy in the immunity of tumors becomes all the more important when dissecting the phenotype of tumor cellularity after treatment. Current evidence suggests that $CD8^+$ T cells, which are known to drive anti-tumor responses and $CD4^+CD25^{hi}FOXP3^+$ regulatory T cells (Treg), known to suppress anti-tumor responses are associated with disease prognosis respectively. Although $CD8^+$ T cells accumulate at tumor sites, the number of Treg present limits their efficacy. This ratio is prognostically significant and as such, is an important determinant in the efficacy of therapy against a particular tumor.[38]

In order to assess this against both Polymer 1 and CPT, treated cells were stained with Propidium Iodide (PI) and sorted via flow cytometry. Those that were PI-negative were collected and phenotyped for $CD8^+$ (7A) and Treg (7B) populations using flow cytometry. As with the cell proliferation data, there were distinct changes in each cell population, when stimulation was provided or omitted. Stimulation, either through antigen introduction, immunotherapeutic induction or enhanced growth factor availability, leads to $CD8^+$ cell proliferation, which would render them more sensitive to cytotoxic chemotherapeutics.

Interestingly, significant differences in $CD8^+$ T cell populations were documented in groups treated with Polymer 1 compared to those treated with CPT (Figure 7C). $CD8^+$ T cells were refractory to depletion when treated with Polymer 1, compared to CPT treatment where extensive depletion occurred in a dose dependent manner ($p < 0.05$). This suggested that Polymer 1 left the CD8+ T cell compartment, a crucial inducer of anti-tumor immunity, intact.

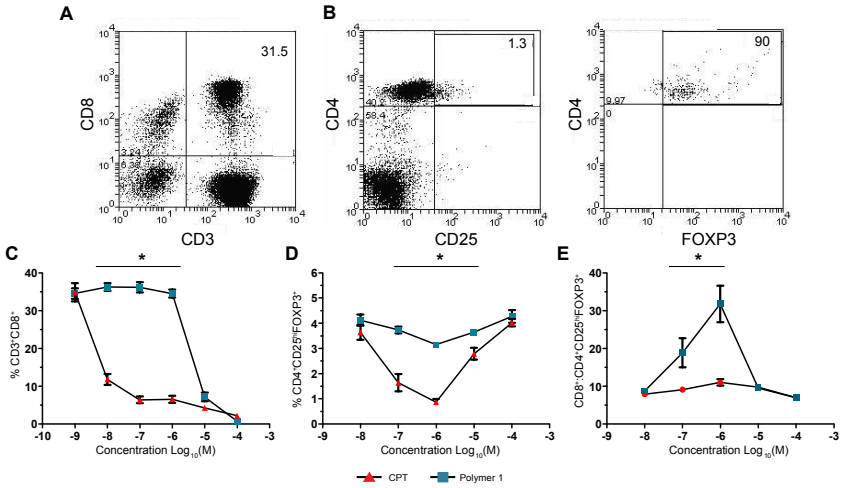

Figure 7. Phenotypic analysis of PHA-stimulated PBMC with Polymer 1(■) and CPT (▲). (A) $CD3^+CD8^+$ T cells and (B) Treg (% of Treg was calculated by determining the number of $CD4^+CD25^{hi}$ cells that were also $FOXP3^+$). Cells treated over a concentration range of 0 – 100 µM. (C) $CD3^+CD8^+$ T cells, (D) Treg. (E) Ratio of $CD8^+$ to Treg. Figures representative of three independent experiments. Error bars represent standard deviation. Statistical significance determined by a one-way ANOVA analysis with column comparisons using Tukey's Multiple Comparison Test (* = $p < 0.05$).

Furthermore, analysis of Treg when treated with Polymer 1 demonstrated a subtle, but significant, decrease in the proportion of these cells. To support this, a significant, more pronounced, decrease in Treg population was demonstrated with cells treated with CPT (Figure 7D). Treg depletion appeared to occur within a narrow therapeutic window (0.1 - 10 µM), thus conforming with observations seen with other cytotoxic agents.[39] Crucially, when determining the ratio of $CD8^+$ T cells to Treg, Polymer 1 demonstrated a significantly higher ratio compared to CPT. This reveals a unique property of Polymer 1 which is to have tumor-specific activity, yet aid

immunological clearance of the tumor through maintenance of anti-tumor effector T cells.

Conclusions

Several chemotherapeutics that are commonly used in the treatment of malignant disease have off-target effects on many tissues and organs. It is therefore essential to minimize these effects while maintaining cytotoxic efficacy. Polymer-based formulations have been shown to improve the specificity and pharmacodynamics of cytotoxic drugs. However the conjugation of a drug to a polymer normally causes a significant loss in activity of the drug while the loading efficiency is often low. Here, we have demonstrated the synthesis and evaluation of a novel targeted polymer therapeutic, which self-assembled into a targeted nanoparticle drug delivery system and demonstrated site-specific release.

We synthesized a polymer prodrug using a living radical polymerization technique and a polymerizable CPT drug moiety containing a reducible linker. By adopting this strategy we were able to create a polymer prodrug that had high drug loading and a tailored polymer structure which further shielded the CPT. The targeting of the CPT into cancer cell lines was achieved by modifying the surface of the polymer micelle with a LHRH peptide sequence. The micelle was successfully taken up into LHRHR positive cells line via the receptor and the prodrug displayed comparable cytotoxicity to the free CPT after 72 hours. In cell lines, which had lower levels of LHRHR expression, and in a LHRHR negative cell line the polymer prodrug displayed significantly lower cytotoxicity in comparison to the free drug. The polymer prodrug self assembled into discrete 40 nm diameter objects in physiological buffer which is considered to be within the optimal range for a drug delivery vehicle.[40]

A caveat of many early studies into polymer therapeutics, both *in vitro* and *in vivo* is that they do not factor in the immunological component i.e. athymic, immune-deficient mice are used for cancer modeling and cytotoxicity assessment.[41] These models may function to demonstrate the cytotoxicity of therapy toward the tumor but fail to account for the intricate role the immune system plays in tumor development or tumor clearance. Therefore it is important at an early stage to screen whether polymer-based therapeutics can also influence events at an immunological level in comparison to the free drug, as the immunological effects can also determine the clinical outcome. We therefore examined the effects our conjugate had on peripheral blood immune populations, with particular focus on T cell subsets, and compared them to that of the native CPT. Despite its tumoricidal activity, it is clear that CPT demonstrates indiscriminate toxicity against the immune system, with impairment of PBMC proliferation and a reduction in $CD8^+$ T cell populations. Polymer 1 appears to limit these effects, with improvements in cell proliferation and maintenance of $CD8^+$ T cells. An interesting observation was the reduction in the immune suppressive Treg cell subset. Specific doses of cytotoxics such as Cyclophosphamide have previously demonstrated the ability to reduce the proportion of Treg from peripheral blood.[42] We have been able to show that within a narrow dosing window CPT can also reduce Treg populations. This effect is replicated, although less dramatically, with Polymer 1. What makes this observation of further interest is that PBMC treated with Polymer 1 consist of a greater $CD8^+$/Treg ratio (e.g. high % $CD8^+$ and low % Treg) compared to those treated with CPT (low % $CD8^+$ and low % Treg). Current prognostic data suggests that this would be of benefit within the ovarian tumor microenvironment as a reduction in tumor burden, combined with an increase in $CD8^+$:Treg ratio would lead to a greater opportunity for tumor clearance.[24,42] It could therefore be argued that tumor directed polymer drug delivery systems could provide therapeutically selective lymphopenia, allowing regeneration of the tumor microenvironment with uninhibited immune populations whilst attenuating peripheral immune toxicity.

Acknowledgements

This article is dedicated in memory of Prof. Sue Watson of Pre-Clinical Oncology, University of Nottingham who passed away in November 2011. Dr. James Hair of MedImmune is thanked for his time and input in the manuscript. This work was funded by EPSRC Grants EP/D501849/1, EP/I01375X/1 (Centre for Doctoral Training in Targeted Therapeutics), an EPSRC Leadership Fellowship - EP/H005625/1 to CA, and AstraZeneca.

Notes and references

a –School of Pharmacy, University of Nottingham, University Park, Nottingham NG7 2RD, UK. e-mail: Cameron.alexander@nottingham.ac.uk, Johannes.magnusson@nottingham.ac.uk

b – Pre-Clinical Oncology, School of Medical and Surgical Sciences, Queens Medical Centre, University of Nottingham, NG7 2UH.

c – Cancer Infection Research Area, AstraZeneca, Alderley Park, Cheshire, SK10 4TG and MedImmune, Aaron Klug Building, Granta Park, Cambridge, CB21 6GH, UK

d- Translational Immunology Group, School of Medicine, Trinity College Dublin, Dublin, Dublin 2, Ireland, . e-mail: Adnan.Khan@tcd.ie.

The authors declare no competing financial interest.

Electronic Supplementary Information (ESI) available: [Reaction scheme for initiator and Camptothecin monomer. ^{1}H-NMR spectra of polymers. DLS analysis, critical aggregation concentration (CAG) of block copolymer, drug release data and Transmission electron microscropy]. See DOI: 10.1039/b000000x/

1. R. Duncan and R. Gaspar, *Molecular Pharmaceutics*, 2011, **8**, 2101-2141.
2. V. Delplace, P. Couvreur and J. Nicolas, *Polymer Chemistry*, 2014, **5**, 1529-1544.
3. X. C. Yang, B. Samanta, S. S. Agasti, Y. Jeong, Z. J. Zhu, S. Rana, O. R. Miranda and V. M. Rotello, *Angew. Chem.-Int. Edit.*, 2011, **50**, 477-481.
4. C. Boyer and T. P. Davis, *Polymer Chemistry*, 2014, **5**, 1501-1502.
5. A. H. A. Mohamed-Ahmed, K. A. Les, S. L. Croft and S. Brocchini, *Polymer Chemistry*, 2013, **4**, 584-591.
6. R. Duncan, *Current Opinion in Biotechnology*, 2011, **22**, 492-501.
7. G.-Y. Liu, L.-P. Lv, C.-J. Chen, X.-S. Liu, X.-F. Hu and J. Ji, *Soft Matter*, 2011, **7**, 6629-6636.

8. H. Maeda, H. Nakamura and J. Fang, *Advanced Drug Delivery Reviews*, 2013, **65**, 71-79.
9. H. Maeda, J. Wu, T. Sawa, Y. Matsumura and K. Hori, *Journal of Controlled Release*, 2000, **65**, 271-284.
10. S. Biswas, N. S. Dodwadkar, P. P. Deshpande and V. P. Torchilin, *Journal of Controlled Release*, 2012, **159**, 393-402.
11. M. J. Demeure, E. Stephan, S. Sinari, D. Mount, S. Gately, P. Gonzales, G. Hostetter, R. Komorowski, J. Kiefer, C. S. Grant, H. Han, D. D. von Hoff and K. J. Bussey, *Annals of Surgery*, 2012, **255**, 140-146.
12. J. Sanchis, F. Canal, R. Lucas and M. J. Vicent, *Nanomedicine*, 2010, **5**, 915-935.
13. J. Khandare and T. Minko, *Progress In Polymer Science*, 2006, **31**, 359-397.
14. R. Satchi-Fainaro, R. Duncan and C. M. Barnes, in *Polymer Therapeutics II: Polymers As Drugs, Conjugates And Gene Delivery Systems*, Springer, Berlin Heidelberg, 1st edn, 2006, vol. 193, pp. 1-65.
15. N. Larson and H. Ghandehari, *Chemistry Of Materials*, 2012, **24**, 840-853.
16. B. M. Blunden, D. S. Thomas and M. H. Stenzel, *Polymer Chemistry*, 2012, **3**, 2964-2975.
17. T. M. Allen and P. R. Cullis, *Science*, 2004, **303**, 1818-1822.
18. V. P. Torchilin, *Nature Reviews Drug Discovery*, 2005, **4**, 145-160.
19. B. E. Rolfe, I. Blakey, O. Squires, H. Peng, N. R. B. Boase, C. Alexander, P. G. Parsons, G. M. Boyle, A. K. Whittaker and K. J. Thurecht, *Journal of the American Chemical Society*, 2014, **136**, 2413-2419.
20. T. Lammers, F. Kiessling, W. E. Hennink and G. Storm, *Journal of Controlled Release*, 2012, **161**, 175-187.
21. Y. H. Bae and K. Park, *Journal of Controlled Release*, 2011, **153**, 198-205.
22. N. M. Zaki and N. Tirelli, *Expert Opinion on Drug Delivery*, 2010, **7**, 895-913.
23. T. G. Burke and Z. Mi, *Journal of Medicinal Chemistry*, 1994, **37**, 40-46.
24. J. Dancey and E. A. Eisenhauer, *British Journal of Cancer*, 1996, **74**, 327-338.
25. F. M. Muggia, O. S. Selawry, H. H. Hansen, P. J. Creaven and M. H. Cohen, *Cancer Chemotherapy Reports Part 1*, 1972, **56**, 515-521.
26. K. Matyjaszewski, *Macromolecules*, 2012, **45**, 4015-4039.
27. S. S. Dharap, Y. Wang, P. Chandna, J. J. Khandare, B. Qiu, S. Gunaseelan, P. J. Sinko, S. Stein, A. Farmanfarmaian and T. Minko, *Proceedings of the National Academy of Sciences of the United States of America*, 2005, **102**, 12962-12967.
28. P. Volker, C. Grundker, O. Schmidt, K. D. Schulz and G. Emons, *American Journal of Obstetrics and Gynecology*, 2002, **186**, 171-179.
29. S. S. Dharap and T. Minko, *Pharmaceutical Research*, 2003, **20**, 889-896.
30. J. P. Magnusson, S. Bersani, S. Salmaso, C. Alexander and P. Caliceti, *Bioconjugate Chemistry*, 2010, **21**, 671-678.
31. M.-J. Li, C. Jiang, M.-Z. Li and T.-P. You, *Journal of Molecular Structure: THEOCHEM*, 2005, **723**, 165-170.
32. X. Zhang and K. Matyjaszewski, *Macromolecules*, 1999, **32**, 7349-7353.
33. J. E. Gestwicki, C. W. Cairo, L. E. Strong, K. A. Oetjen and L. L. Kiessling, *Journal of the American Chemical Society*, 2002, **124**, 14922-14933.
34. G. C. Gründker, A. R. Günthert, R. P. Millar and G. Emons, *Journal of Clinical Endocrinology and Metabolism* **2002**, *87*, 1427–30.
35. J. P. Hapgood, H. Sadie, W. Van Biljon and K. Ronacher, *Journal of Neuroendocrinology* **2005**, *17*, 619–38.
36. J. Dey and I. M. Warner, *Journal of Luminescence*, 1997, **71**, 105-114.
37. N. M. Blackett and K. Adams, *British Journal of Haematology*, 1972, **23**, 751-758.
38. W. P. Zou, *Nature Reviews Cancer*, 2005, **5**, 263-274.
39. S. Sakaguchi, M. Miyara, C. M. Costantino and D. A. Hafler, *Nature Reviews Immunology*, 2010, **10**, 490-500.
40. L. Qiu and Y. Bae, *Pharmaceutical Research*, 2006, **23**, 1-30.
41. G. Dranoff, *Nature Reviews Immunology*, 2012, **12**, 61-66.
42. F. Ghiringhelli, N. Larmonier, E. Schmitt, A. Parcellier, D. Cathelin, C. Garrido, B. Chauffert, E. Solary, B. Bonnotte and F. Martin, *European Journal of Immunology*, 2004, **34**, 336-344.